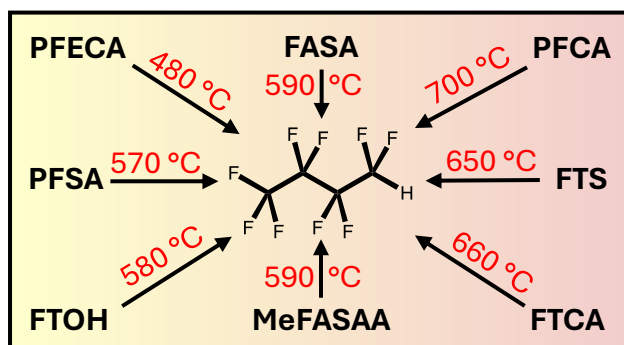


Head Group Dependence and Kinetic Bottlenecks of Gas-phase Thermal PFAS Destruction

Jens Blotevogel¹, Justin P. Joyce², Olivia L. Hill², Anthony K. Rappé^{2,*}

¹ CSIRO, Environment, Waite Campus, Urrbrae, SA 5064, Australia

² Department of Chemistry, Colorado State University, Fort Collins, CO 80523, USA



TOC Art

KEYWORDS: AFFF, PFOS, PFOA, incineration, combustion, pyrolysis

1 ABSTRACT

2 Varying and sometimes conflicting temperatures and products have been reported from
3 studies addressing thermal PFAS destruction, often because decomposition pathways are highly
4 dependent on the respective experimental system. Here we applied highest-level coupled cluster
5 calculations to isolate and identify the major processes during thermal PFAS destruction in the gas
6 phase with relevance to incineration, thermal oxidation, and other thermal treatment technologies
7 in which PFAS and their volatile decomposition products desorb into the gas phase. All
8 investigated perfluoroalkyl acids decompose via unimolecular head group loss, either through HF
9 elimination or homolytic bond cleavage as a function of head group type. In contrast, all
10 investigated fluorotelomers undergo initial hydrogen abstraction from the characteristic C₂H₄
11 moiety by hydroxyl radicals under representative incineration conditions, followed by radical
12 decomposition. Subsequent formation of perfluoroalkanes including CF₄ can then be prevented by
13 supplying sufficient hydrogen donors such as hydrocarbon fuel and water as well as by scavenging
14 released fluorine. This leads to the generation of stable 1*H*-perfluoroalkanes. While parent PFAS
15 decomposition proceeds at gas-phase temperatures ≤ 700 °C, carbon-carbon cleavage of 1*H*-
16 perfluoroalkanes requires up to ~ 950 °C at 2 seconds gas residence time, making this step the
17 kinetic bottleneck on the way to complete thermal PFAS mineralization.

18

19 SYNOPSIS

20 Concerns exist around PFAS stack emissions. This study identifies the main decomposition
21 pathways and conditions needed for complete thermal gas-phase destruction of eleven major PFAS
22 classes.

23 INTRODUCTION

24 Per- and polyfluoroalkyl substances (PFAS) comprise well over 10,000 individual
25 chemicals that are used in countless commercial, industrial, and consumer products.^{1,2} While the
26 composition and properties of their head groups vary greatly with their respective type of
27 application, the functional group common to all PFAS is a perfluoroalkyl tail.³ This remarkably
28 unreactive functional group is the root of PFAS' high persistence both in the environment and in
29 traditional water, soil, and waste treatment technologies.⁴

30 Thermal destruction is among the few treatment processes that can break the strong carbon-
31 fluorine bond and completely mineralize PFAS.⁵ However, as the scientific community's
32 understanding of high-temperature fluorocarbon chemistry is still evolving, concerns about stack
33 emissions of potentially toxic products of incomplete destruction (PIDs) persist.⁶ This lack of
34 understanding has led to great uncertainty within the regulatory community, and as a consequence
35 to widely varying regulations internationally to the point of temporary prohibition of incineration
36 of PFAS-containing materials in the U.S.^{7,8}

37 Adding to the uncertainties around thermal PFAS destruction are observations that, at first
38 glance, may seem contradictory. For instance, Xiao and co-workers (2020)⁹ found that
39 perfluoroalkane sulfonic acids (PFSAs) needed a higher decomposition temperature than
40 perfluoroalkyl carboxylic acids (PFCAs) during treatment of spent granular activated carbon
41 (GAC). In contrast, Shields et al. (2023)¹⁰ reported higher destruction efficiencies for PFSAs
42 compared to PFCAs during the incineration of aqueous film forming foam (AFFF) in a pilot-scale
43 research combustor. Likely reasons for these discrepancies are (1) surface catalytic processes that
44 are highly material-specific and fundamentally different from gas phase processes as well as (2)
45 concurrent volatilization processes that are captured as mass loss during thermogravimetric

46 analysis but do not necessarily reflect partial or complete destruction of the analytes.⁶ Furthermore,
47 both Shields et al. (2023)¹⁰ and Mattila et al. (2024)¹¹ observed a decrease in PFCA destruction
48 efficiency with decreasing fluorocarbon chain length, while we witnessed only little chain length
49 dependence in PFCA head group loss in a previous computational study.¹² A possible explanation
50 for this disagreement between physical and theoretical experiments could be the generation of
51 shorter-chained PFCAs and therefore an apparent decrease in their destruction efficiency during
52 concurrent thermal destruction of longer-chained PFAS. Clearly, more mechanistic insights are
53 needed to unravel the underlying processes and kinetics in complex mixtures.

54 To systematically start identifying and characterizing the highly complex field of thermal
55 PFAS destruction, our study is aimed at elucidating the fundamental steps in the gas phase.
56 Gaseous transformation pathways, mechanisms, and kinetics are not only relevant for assessing
57 PFAS fate in incinerators and thermal oxidizers, but likely also for other thermal processes such
58 as GAC reactivation and pyrolysis of impacted biosolids, where PFAS decomposition may be
59 initiated on a potentially catalytically active surface, but where highly volatile fluorocarbon
60 intermediates may only be mineralized after desorption into the gas phase.^{13,14} To exclude any
61 surface reaction bias from physical experiments and to overcome the lack of analytical methods
62 capable of detecting often short-lived key intermediates in the thermal decomposition of PFAS,
63 we applied highly accurate quantum chemical calculations using coupled cluster with single and
64 double and perturbative triple excitations (CCSD(T)), which we previously benchmarked against
65 data from physical experiments to confirm that our predictions can achieve chemical accuracy (± 1
66 kcal/mol).¹² While CCSD(T) calculations are computationally expensive, their use in the
67 investigation of fluorine chemicals is justified because less costly density functional theory (DFT)
68 methods struggle with accurately describing non-covalent interactions, excited states, and kinetic

69 descriptors such as activation barriers.¹⁵ Accurate quantification of activation barriers is especially
70 important in high-temperature systems where homolytic bond cleavage proceeds through a
71 variational transition state and, in contrast to ambient temperature, cannot be kinetically described
72 by a bond dissociation (free) energy.^{12,16-18}

73 The first specific objective of our study was to determine the head group dependence on
74 thermal PFAS destruction. Head group loss is thought to be the first step in high-temperature
75 decomposition of PFAS and therefore determines a parent compound's destruction efficiency, a
76 descriptor widely used to benchmark the effectiveness of incineration processes.^{10,19,20} Thus far,
77 mechanistic studies have exclusively focused on head group loss in PFCAs and PFSAAs.^{12,18,21-23}
78 Some of these studies disagree over the primary decomposition mechanism, partly because of the
79 disregard of variational transition states. Here, we aim to settle these disagreements and expand
80 our mechanistic understanding to a broader set of PFAS head groups that have not been
81 investigated yet, such as sulfonamides, telomers, and alcohols. However, as destruction efficiency
82 does not necessarily relate to complete mineralization of an organic chemical,⁶ the second specific
83 objective of our study was to identify the kinetic bottleneck for thermal PFAS mineralization in
84 the gas phase. Collectively, we envision these results to provide a framework for safe and efficient
85 thermal destruction of these highly persistent environmental contaminants.

86

87 **COMPUTATIONAL DETAILS**

88 All gas-phase computations were performed on uncharged (acid) species. As previously
89 described,¹² reported ground and transition state geometry optimizations as well as vibrational
90 frequency computations used the 6-311+G(2d,2p) basis set,²⁴ the ω B97X-D hybrid functional,²⁵
91 an unrestricted formalism for radical species, and the Gaussian 16 electronic structure package.²⁶

92 Single point computations were carried out at stationary points using the aug-cc-pVTZ basis set^{27,28}
93 and the DLPNO-CCSD(T) coupled cluster approach^{29,30} in the ORCA suite of programs.³¹ The
94 aug-cc-pVTZ basis for sulfur-containing compounds was augmented with a tight *d* exponent of
95 3.203.³² Estimates of variational transition state free energies of activation $\Delta^\ddagger G$ were obtained
96 along constrained bond dissociation curves.¹⁷ The maximum $\Delta^\ddagger G$ required to achieve 99%
97 destruction in 2 seconds of combustion gas residence time (t_{99}) curve was obtained along
98 constrained bond dissociation curves to calculate T_{99} temperatures, a common laboratory
99 benchmark indicative of 99.99% destruction and removal efficiency (DRE) at full scale.¹⁹ To
100 describe representative incineration conditions, partial pressures for incineration accrued from
101 estimated initial partial pressures for O₂, H₂O, and methane of 18.3% and 8.5%, and 4.25%,
102 respectively. These initial concentrations were used in Cantera³³ to provide temperature-dependent
103 equilibrium concentrations and associated free energy corrections for bimolecular reactions with
104 second-order kinetics (Fig. S1, Tables S1-S3). Additional details are provided in the Supporting
105 Information.

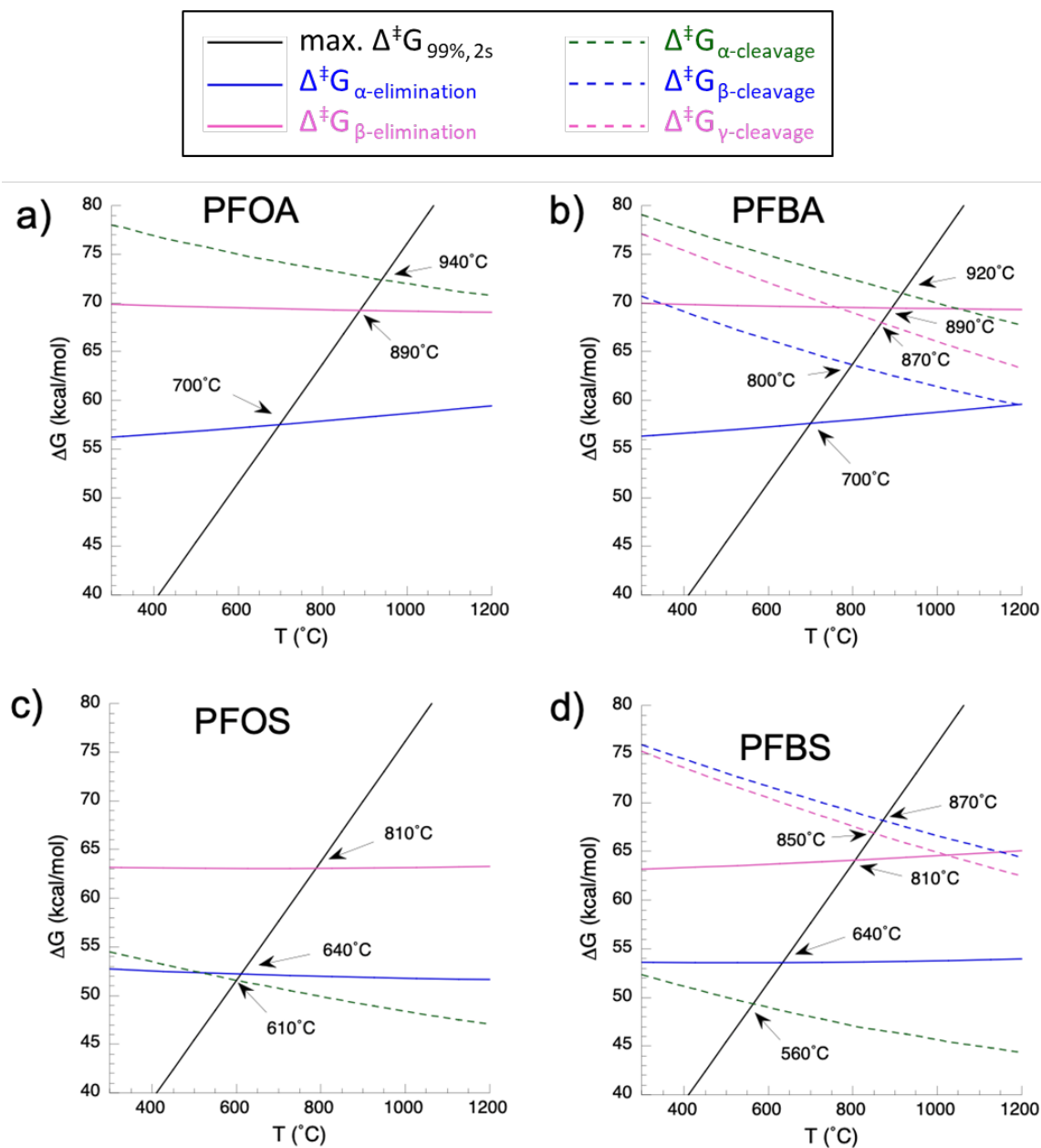
106 As 1 kcal/mol is roughly equivalent to 17 °C within the range of incineration temperatures,
107 we estimate that the error of our T_{99} temperatures is within ± 20 °C.

108

109 RESULTS AND DISCUSSION

110 **Unimolecular Head Group Loss.** Initial PFAS head group loss can proceed via unimolecular or
111 bimolecular reactions. Unimolecular mechanisms include hydrogen fluoride (HF) elimination and
112 homolytic bond dissociation.^{6,34} Starting with carboxylic acids, Fig. 1 shows that HF elimination
113 at the α -carbon (“ α -elimination”) requires the lowest temperature among these mechanisms in
114 perfluorooctanoic acid (PFOA) and perfluorobutanoic acid (PFBA), meaning it is the kinetically

115 most favorable unimolecular decomposition pathway for these two PFCAs consistent with
116 previous studies.^{12,18} In PFBA, cleavage of the β C-C bond is favored over cleavage of the α and
117 γ C-C bonds (Figure 1b, Table S4), in agreement with bond dissociation energy estimates by
118 Alinezhad and co-workers.³⁵ The free energy barrier $\Delta^\ddagger G$ for HF elimination is almost independent
119 of temperature as there is very little entropy change in the rearrangement, while the barrier for
120 homolytic C-C cleavage decreases notably with increasing temperature due to transitional entropy
121 build-up. The computed T_{99} of 700 °C for PFOA based on the preferred mechanism α -elimination
122 agrees well with the equivalent temperature of 680 °C from physical experiments by Weber and
123 co-workers, who carefully vaporized PFOA before inducing its thermal decomposition.³⁶
124 Branching of the perfluorocarbon chain lowers the required temperatures for all three mechanisms
125 by up to 190 °C for C-C cleavage, although α -elimination remains the kinetically most favorable
126 pathways for branched PFOA ($T_{99} = 650$ °C, Table 1). The product of α -elimination during gas-
127 phase PFCA decomposition is an acyl fluoride (R-COF, Table 1).^{12,18,37} This product distribution
128 may differ in the presence of solid surfaces, where the alkene products from β -elimination have
129 been observed in physical experiments.^{34,38} The perfluoroalkylether carboxylic acid (PFECA)
130 hexafluoropropylene oxide dimer acid (HFPO-DA, a.k.a. “GenX”) likewise decomposes via α -
131 elimination in the gas phase at a substantially lower T_{99} of 480 °C compared to PFCAs.¹²



132

133 **Figure 1. Free energies of activation as a function of temperature for α -HF elimination, β -**

134 **HF elimination, and homolytic C-C bond cleavage for PFOA (a) and PFBA (b) or C-S bond**

135 **cleavage for PFOS (c) and PFBS (d). The black line illustrates the maximum free energy of**

136 **activation required to achieve 99% destruction in 2 seconds of combustion gas residence time**

137 **(t_{99}). The temperatures at the crossing points of the respective lowest free energy of activation**

138 **and the black line represent T_{99} .**

139 Recent computational studies have reported α -elimination via sultone formation to be the
140 primary pathway for head group loss in PFSAAs.^{22,23} However, the emergence of variational
141 transition states at elevated temperature has been neglected for PFSAAs thus far, and many previous
142 computational studies have been carried out at zero Kelvin.⁶ Our highly accurate computations,
143 which were carried out over a temperature range of 1 to 2000 Kelvin, reveal that α -elimination is
144 indeed the primary head loss mechanism for perfluorooctane sulfonic acid (PFOS) and
145 perfluorobutane sulfonic acid (PFBS), but only at temperatures below 520 °C and 190 °C,
146 respectively (Fig. 1). Above these temperatures, the relatively weak C-S bond leads to a curve
147 crossing and for the homolytic C-S cleavage path to be preferred. The products of initial C-S bond
148 cleavage in PFSAAs are a perfluoroalkyl radical and HSO₃, which can reductively or oxidatively
149 form H₂SO₃ or H₂SO₄. The T_{99} values of 610 °C for PFOS and 560 °C for PFBS are lower than
150 for PFOA and PFBA, which is consistent with the weaker C-S bond for PFSAAs compared to the
151 C-C bond of PFCAs. Our computational findings are supported by recent physical experiments
152 where the favored product formation pathway is observed to be temperature-dependent.³⁹ It should
153 be noted that, on average, the T_{99} for C-C cleavage was underestimated by 100 °C using DFT (here
154 ω B97xd) compared to highly accurate DLPNO-CCSD(T).

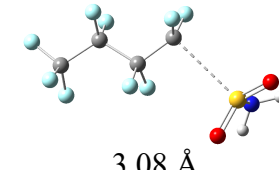
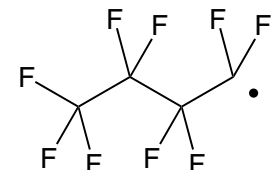
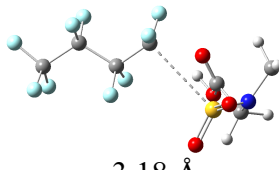
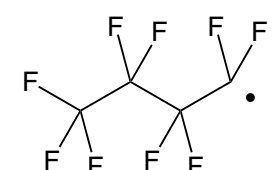
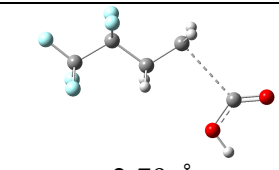
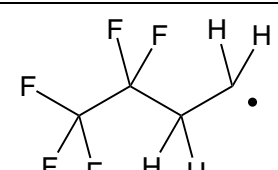
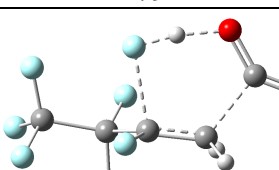
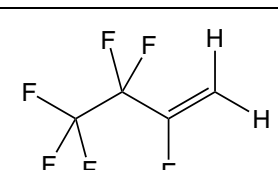
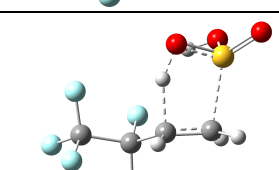
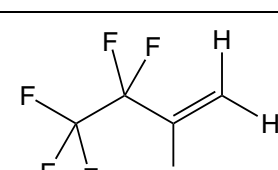
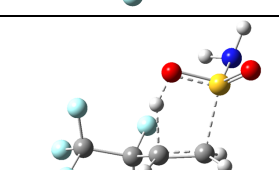
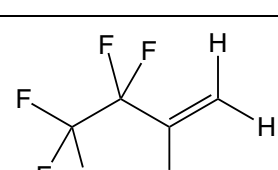
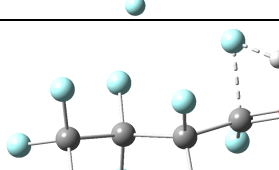
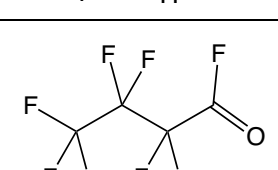
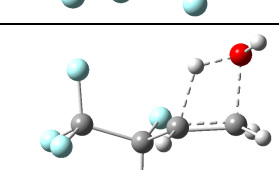
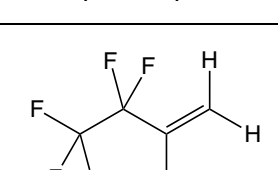
155 **Table 1. Unimolecular head group loss pathways with calculated T_{99} temperatures. The**
 156 **asterisk (*) indicates the favored unimolecular decomposition pathway for each PFAS.**

Substrate	α -Elimination	Geometries of the kinetically most favorable transition state incl. bond distance for variational transition states during cleavage	Product of initial unimolecular head group loss
	β -Elimination		
	α -Cleavage		
PFOA (linear)	700 °C *		
	890 °C		
	940 °C		
PFOA (branched)	650 °C *		
	810 °C		
	750 °C		
PFBA	700 °C *		
	890 °C		
	920 °C		
HFPO-DA ("GenX")	480 °C *		
	860 °C		
	890 °C		
PFOS	640 °C		
	810 °C		
	610 °C *		
PFBS	640 °C		
	810 °C		
	560 °C *		

157

158

159 **Table 1 (continued).**

FBSA	1030 °C	 3.08 Å	
	1060 °C		
	590 °C *		
<i>N</i> -MeFBSAA	not applicable	 3.18 Å	
	not applicable		
	590 °C *		
2:3 FTCA	950 °C	 2.79 Å	
	1120 °C		
	880 °C *		
3:2 FTCA	920 °C		
	690 °C *		
	950 °C		
2:2 FTS	950 °C		
	710 °C *		
	740 °C		
2:2 FTSA	840 °C		
	650 °C *		
	700 °C		
PFBOH	470 °C *		
	780 °C		
	840 °C		
2:2 FTOH	1040 °C		
	770 °C *		
	900 °C		

160

161 We note that for both PFCAs and PFSAAs there is little chain length dependence for the
162 initial head group loss. Therefore, shorter chains of two to four perfluorinated carbons were chosen
163 as representative homologues of the remaining investigated PFAS classes to keep computational
164 expenses affordable.

165 Transitioning from a sulfonic acid to the sulfonamide, here perfluorobutane sulfonamide
166 (FBSA), leads to a profound suppression of the α - and β -elimination pathways, as shown in Fig.
167 S2 in the Supporting Information. The T_{99} rises from 640 °C for PFSAAs to over 1000 °C due to the
168 loss of acidity in the amide functional group. For both FBSA and *N*-methylperfluorooctane
169 sulfonamidoacetic acid (*N*-MeFBSAA), C-S cleavage is the kinetically preferred pathway with a
170 T_{99} of 590 °C, only 30 °C higher than for the C₄-PFSA analogue PFBS (Tables 1 and S4). The C-
171 S cleavage pathway leads to the generation of a perfluoroalkyl radical analogous to the chain
172 scission pathway proposed by Xiao and co-workers (2021) based on thermal AFFF decomposition
173 in a muffle furnace.⁴⁰ The alternate N-S cleavage paths are higher at T_{99} values of 800 °C and 610
174 °C for FBSA and *N*-MeFBSAA, respectively, and therefore not favored.

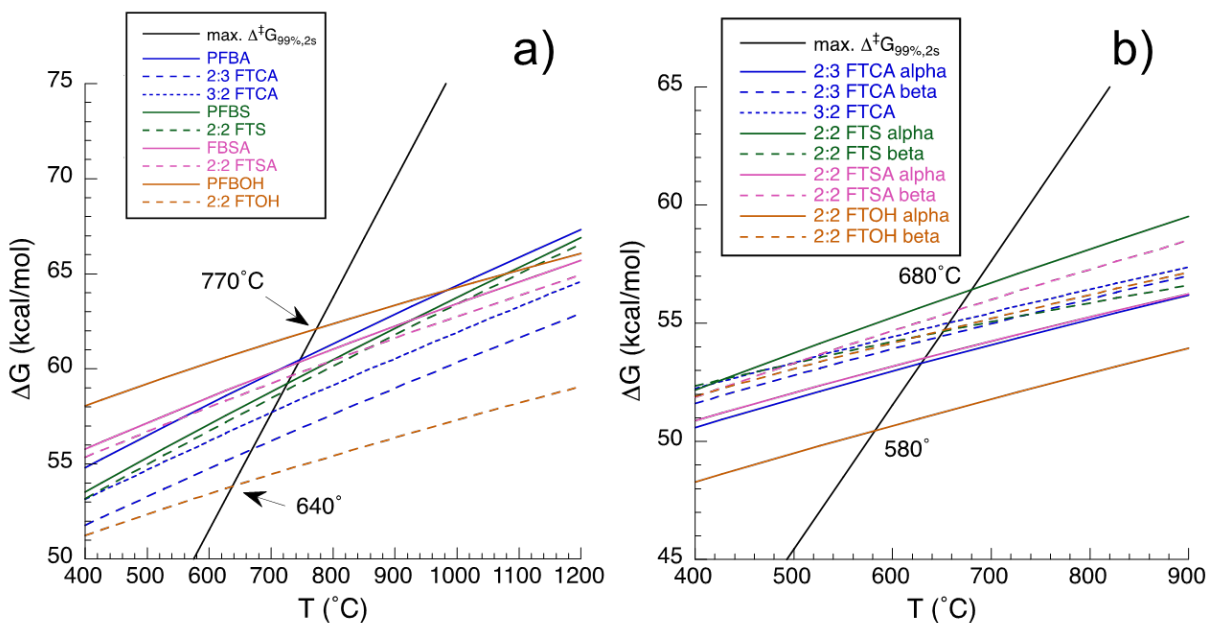
175 In contrast to perfluorinated PFAS, the telomeric C₂H₄ alkyl moiety adjacent to the head
176 group significantly alters the reaction pathways as evident when comparing PFBA to fluorotelomer
177 carboxylic acids (FTCAs) (Table 1). HH elimination is kinetically much less favorable than HF
178 elimination. For 2:3 FTCA, the α - and β -elimination pathways no longer contribute significantly
179 to decomposition and head group elimination parallels that of aliphatic carboxylic acids as
180 summarized in Figs. S3 and S4.⁴¹⁻⁴³ 2:3 FTCA loses its head group through C-C cleavage at a T_{99}
181 values of 880 °C, about 40 °C lower than its non-fluorinated counterpart valeric acid (a.k.a.
182 pentanoic acid).⁴³ 3:2 FTCA, however, has a β -fluorine and preferentially undergoes β -elimination
183 at a T_{99} of 690 °C (Figure S5).

184 In comparison to fluorotelomer carboxylic acids, 2:2 fluorotelomer sulfonic acid (FTS) and
185 2:2 fluorotelomer sulfonamide (FTSA) have lower T_{99} values of 740 °C and 700 °C, respectively,
186 for homolytic cleavage due to a weaker C-S bond. Furthermore, FTSs have a significantly lowered
187 β -elimination barrier relative to FTCAs due to formation of an alkene product and a stabilized
188 S(IV) species ($T_{99} = 710$ °C). For 2:2 fluorotelomer sulfonamide (FTSA), the β -elimination barrier
189 is lowered due to involvement of a C-H bond ($T_{99} = 650$ °C). Consequently, unimolecular
190 decomposition of FTSs and FTSAs will primarily produce an alkene product (Table 1, Fig. S7).

191 Other industrially and commercially relevant fluorotelomers are those with an alcoholic
192 terminal group, here 2:2 fluorotelomer alcohol (FTOH). FTOHs are uncharged, volatile PFAS that
193 readily transform into FTCAs and PFCAs in the environment.⁴⁴ Like FTCAs, α -elimination and
194 bond cleavage pathways are kinetically unfavorable for FTOHs, leading to β -elimination being
195 preferred for unimolecular decomposition ($T_{99} = 770$ °C) and the generation of an alkene
196 intermediate (Table 1). Also like FTCAs, FTOHs undergo head group loss at slightly lower
197 temperatures than their non-fluorinated counterparts (Fig. S8).⁴⁵ Vice versa, the fully fluorinated
198 perfluorobutanol (PFBOH, Fig. S9) loses its head group at a much lower T_{99} of 470 °C through an
199 α -elimination pathway, stabilized by the formation of a carbonyl functional group in contrast to
200 carbene formation for the acids (Table 1).

201 **Radical Abstraction.** Reaction of the parent PFAS with radicals such as $\cdot\text{OH}$, $\text{H}\cdot$, or $\text{R}\cdot$, the latter
202 one for instance stemming from the hydrocarbon fuel, is an alternative to unimolecular
203 decomposition. As shown in Fig. S10, F atom abstraction from PFAS is unfavorable under
204 representative incineration conditions^{12,20} with T_{99} values ranging between 1060 °C for F atom
205 abstraction by hydrogen and 1710 °C for F atom abstraction by fluorine radicals, which may be
206 present from the thermal decomposition of other PFAS in the treated material. With a T_{99} range

207 from 640 °C to 770 °C (Fig. 2a), hydrogen atom abstraction from the head group by $\cdot\text{OH}$ is
 208 kinetically more favorable than by $\text{H}\cdot$ (T_{99} range 730 °C to 850 °C) or $\cdot\text{CH}_3$ radicals (T_{99} range 820
 209 °C to 950 °C, Figure S11).



210
 211 **Figure 2. Free energies of activation as a function of temperature for hydrogen abstraction**
 212 **by hydroxyl radicals (a) from the head groups of four perfluoroalkyl substances their**
 213 **respective telomeric analogues and (b) from the telomeric carbons of five different classes.**
 214 **Data were calculated at O_2 concentrations representative of incineration conditions. The**
 215 **black line illustrates the maximum free energy of activation required to achieve 99%**
 216 **destruction in 2 seconds of combustion gas residence time (t_{99}). The temperatures at the**
 217 **crossing points of the respective lowest free energy of activation and the black line represent**
 218 **T_{99} .**

219 For head group H abstraction, there is a clear trend that telomeric polyfluoroalkyl
 220 substances require lower temperatures than their perfluorinated homologues. The resulting head

221 group radical species are highly unstable and rapidly eliminate CO₂, SO₃, SO₂NH, or CF₂O,
222 generating perfluorocarbon radicals with T_{99} values below room temperature (Fig. S12).

223 However, for all five telomer classes investigated here, H abstraction from the telomeric
224 C₂H₄ moiety requires T_{99} temperatures 30 to 100 °C lower than H abstraction from the respective
225 head group (Fig. 2b). For 2:2 FTS, H abstraction from the β -carbon is most favorable, while for
226 the four other species, H abstraction from the α -carbon is most favorable. In fact, when comparing
227 free energies of activation with unimolecular head loss mechanisms, H abstraction from the
228 telomeric C₂H₄ by \cdot OH under incineration conditions is the most favorable decomposition
229 mechanism for all five investigated fluorotelomers 2:2 FTS ($T_{99} = 650$ °C), 2:2 FTSA ($T_{99} = 630$
230 °C), 2:2 FTOH ($T_{99} = 580$ °C), 3:2 FTCA ($T_{99} = 660$ °C), and 2:3 FTCA ($T_{99} = 630$ °C). Subsequent
231 radical decomposition occurs below 270 °C generating the head group radical and a telomeric
232 alkene (Fig. S13).

233 It is important to note that \cdot OH concentrations are substantially lower under oxygen-
234 depleted conditions, which can exist in poorly mixed incinerators.²⁰ This may lead to an increase
235 in free energies of activation for H abstraction by \cdot OH of 20 kcal/mol (Fig. S1), and consequently
236 to a shift in primary degradation mechanism for fluorotelomers towards other H-abstracting
237 radicals or, as a kinetically worst-case scenario, to the respective primary unimolecular
238 decomposition mechanisms summarized in Table 2.

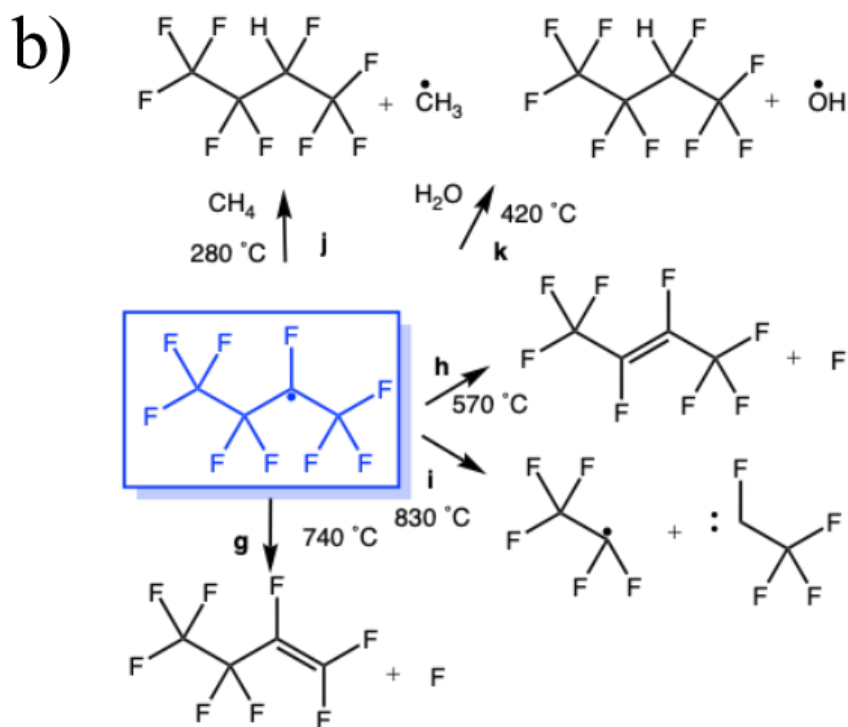
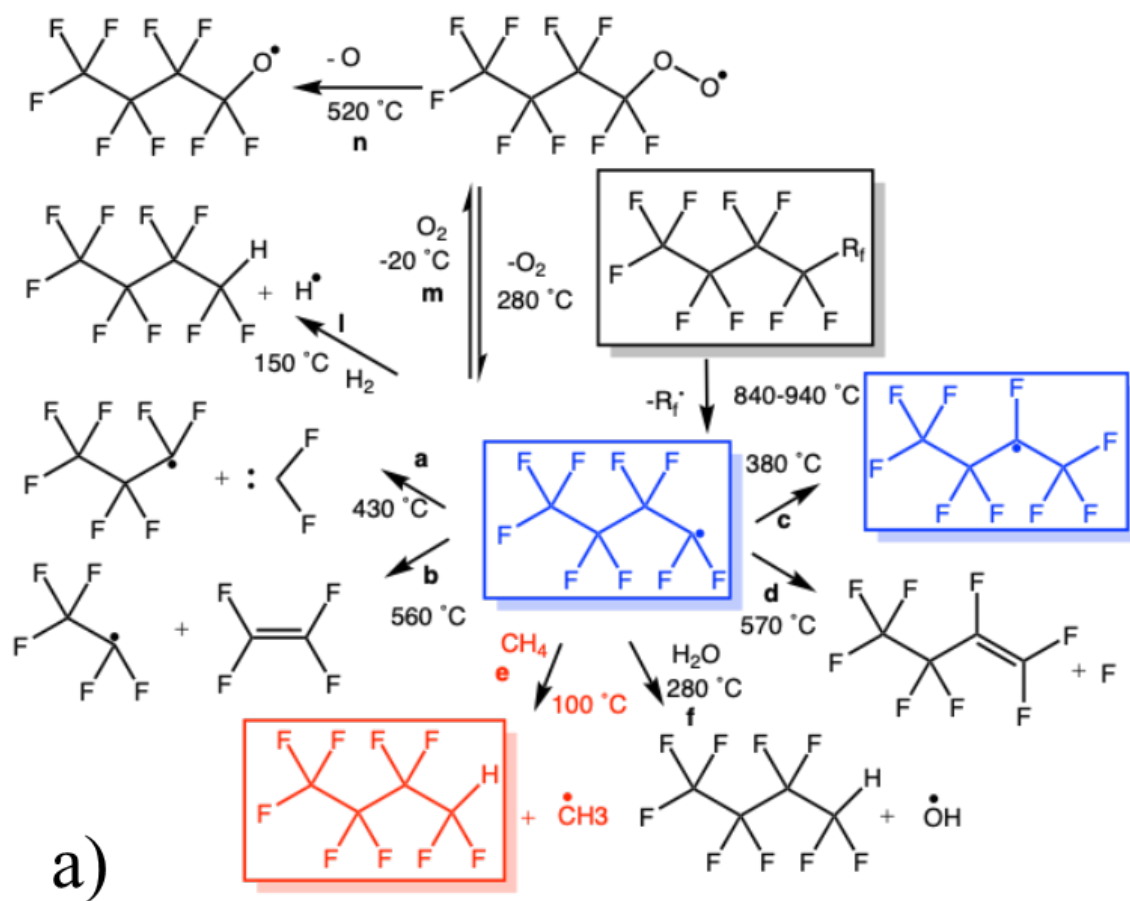
239 **Fate of the Head Group Loss Products.** Once the headgroup has been removed from PFAS, the
240 resulting perfluoroalkyl radicals, acyl fluorides or alkenes can react with abundant gas-phase
241 species such as H₂O, O₂, hydrogen, or hydrocarbon fuel. Alkenes react with H \cdot , \cdot OH, and O₂ at T_{99}
242 temperatures ranging from 610 °C to 740 °C (Fig. S14). Acyl fluorides do not hydrolyze in the gas

243 phase even in the presence of water vapor, but C-C cleavage reactions occur between 830-880 °C
244 and OH addition proceeds between 820-920 °C (Fig. S15 and additional computations below).

245 Perfluoroalkyl radicals can follow several decomposition pathways.^{36,46} Decomposition
246 can form shorter chain perfluoroalkyl radicals and a difluoro carbene CF₂ (pathway **a** in Fig. 3a,
247 $T_{99} = 430$ °C) or tetrafluoroethene C₂F₄ (**b**, $T_{99} = 560$ °C). In contrast, for telomeric fluoroalkyl
248 radicals, ethylene loss ($T_{99} = 290$ °C) is substantially more kinetically favorable than methylene
249 loss ($T_{99} = 1080$ °C, Fig. S16). Alternatively, the primary radical can lose fluorine, generating an
250 alkene (**d**, $T_{99} = 570$ °C). However, H abstraction is the most favorable mechanism for
251 perfluoroalkyl radicals. In an incinerator with significant hydrocarbon fuel and water vapor, H
252 abstraction from H₂O and H₂ proceeds at T_{99} temperatures of 280 °C (**f**) and 150 °C (**l**),
253 respectively, while a very low T_{99} of 100 °C implies that the hydrocarbon fuel (here: CH₄) is the
254 primary source for perfluoroalkyl radical transformation, forming 1*H*-perfluoroalkanes (**e**).

255 Isomerization of primary perfluoroalkyl radicals to more stable secondary radicals only
256 proceeds with a higher T_{99} of 380 °C (**c**). Secondary radicals may undergo the same reactions as
257 primary radicals, though generally at higher temperatures (Figure 3b). Again, the most favorable
258 pathway is H abstraction from the hydrocarbon fuel (**j**) at a T_{99} of 280 °C.

259 Alternatively, as outlined in Fig. S17 under incineration conditions, perfluoroalkyl radicals
260 can also react with O₂ forming peroxy radicals with a T_{99} of -10 °C but require 520 °C to
261 decompose further. Reverse reaction of the peroxy radicals to perfluoroalkyl radicals is kinetically
262 more favorable than (forward) decomposition with a T_{99} of 280 °C. Parallel to hydrocarbon
263 combustion,^{35,47} polyfluoroalkyl radicals also react with O₂ at low temperature and rearrange to
264 hydroperoxyalkyl radical species (**•**QOOH) at 270 °C and decompose to an alkene plus peroxy
265 radical at 40 °C (Fig. S17).

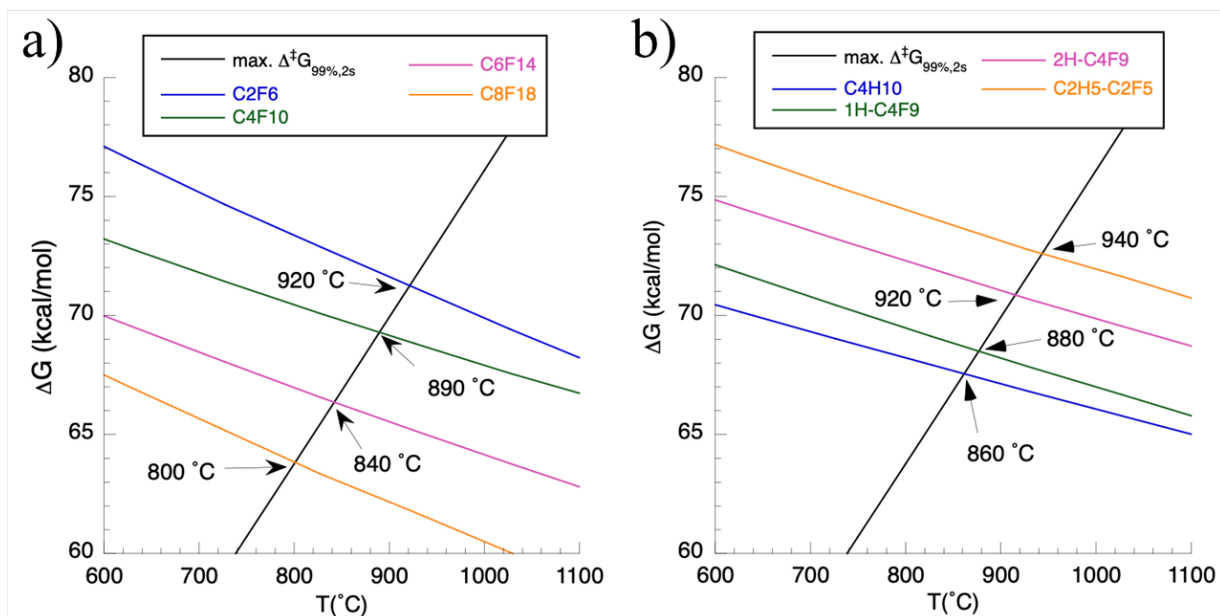


267 **Figure 3. Thermal transformation pathways for (a) primary and (b) secondary**
268 **perfluoroalkyl radicals, both boxed in blue. Perfluoroalkyl radicals are central products of**
269 **head group loss or carbon chain cleavage of larger fluoroalkanes (black box). Temperatures**
270 **provided are T_{99} values. The red T_{99} and red box indicate the kinetically most favorable**
271 **pathway for perfluoroalkyl radicals.**

272 Consequently, various pathways exist for the products of heads group loss with T_{99}
273 temperatures substantially below the temperatures computed for head group removal (Table 1).
274 These products are therefore not the kinetic bottleneck on the path to complete thermal
275 mineralization.

276 **Carbon-Carbon Cleavage in Fluoroalkanes.** While 1*H*-perfluoroalkanes are the predicted major
277 products from perfluoroalkyl radical transformation in treatment systems with excess hydrocarbon
278 fuel, non-hydrogenated perfluoroalkanes may be generated from F trapping/abstraction or
279 recombination of perfluoroalkyl radicals. These fluoroalkanes are thought to decompose via C-C
280 bond dissociation^{46,48} because homolytic cleavage of the carbon-fluorine bond has a substantially
281 higher activation barrier. This is the reason for CF₄ having an exceptionally high T_{99} of 1450 °C.¹²

282 Free energies of activation as a function of temperature for C-C bond cleavage in a series
283 of perfluoroalkanes is shown in Fig. 4a. Both experimental and computational data reveal a general
284 chain length-dependence as required thermal decomposition temperatures increase with
285 decreasing perfluoroalkane size. For the synthetic fluoropolymer polytetrafluoroethylene (PTFE),
286 a T_{99} of only 580 °C has been reported.^{49,50} The required thermal destruction temperatures then
287 increase notably to T_{99} of 800 °C for perfluorooctane, 840 °C for perfluorohexane, and 890 °C for
288 perfluorobutane, until they reach a computationally predicted T_{99} for C₂F₆ of 920 °C, close to the
289 experimentally reported ones of 912 °C,⁵ 919 °C,⁵¹ and 940 °C.⁵²



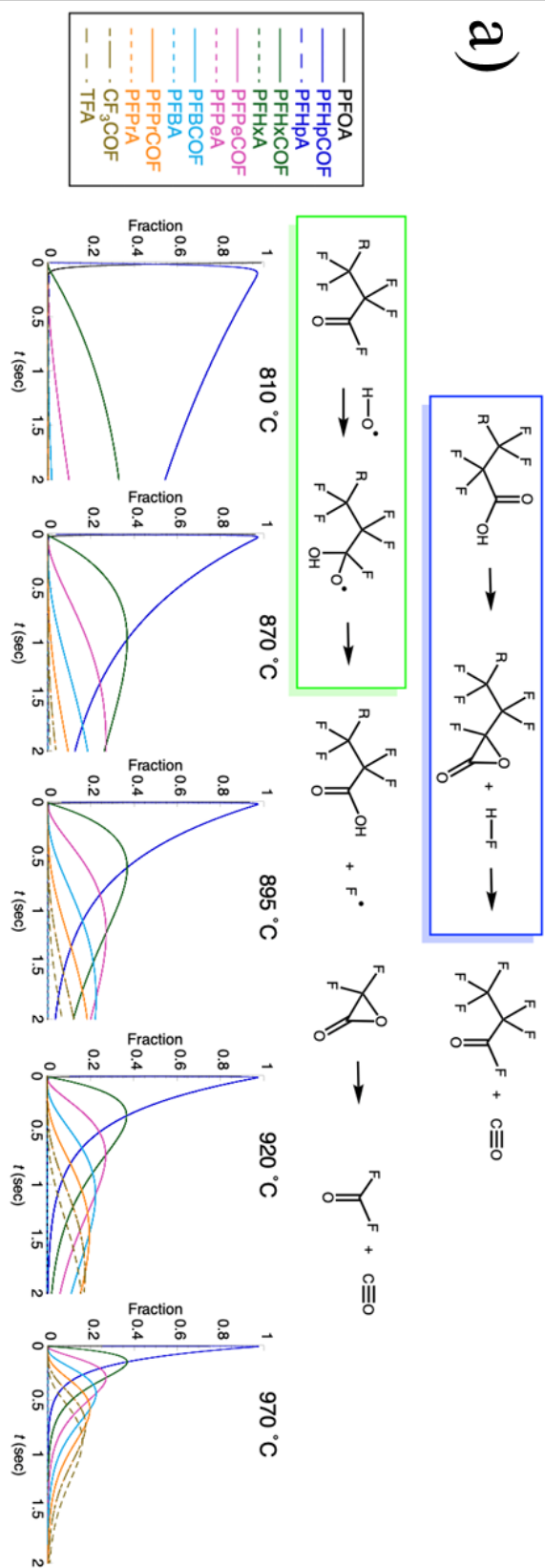
290
 291 **Figure 4. Computed free energies of activation as a function of temperature for C-C bond**
 292 **cleavage in a series of a) perfluoroalkanes and b) butane with varying degrees of fluorination.**
 293 **The black line illustrates the maximum free energy of activation required to achieve 99%**
 294 **destruction in 2 seconds of combustion gas residence time (t_{99}). The temperatures at the**
 295 **crossing points of the respective lowest free energy of activation and the black line represent**
 296 **T_{99} .**

297 The effect of substituting hydrogen for fluorine on C-C bond cleavage T_{99} temperatures
 298 can be seen in the example of C_4 alkanes in Fig. 4b. 1H -perfluorobutane's T_{99} is 880°C , within
 299 the margin of estimation error to perfluorobutane's T_{99} of 890°C . 2H -perfluorobutane's T_{99} is
 300 slightly higher at 920°C , while an alkyl-perfluoroalkyl linkage further raises the temperature to
 301 940°C for $1\text{H},1\text{H},1\text{H},2\text{H},2\text{H}$ -perfluorobutane. For fully hydrogenated (non-fluorinated) butane,
 302 the T_{99} drops to 860°C . Fluorinated C-C bonds are stronger than the hydrogen analog while the
 303 polarity of the heteropolar C-C bond of $\text{C}_2\text{H}_5\text{-C}_2\text{F}_5$ strengthens the bond further.

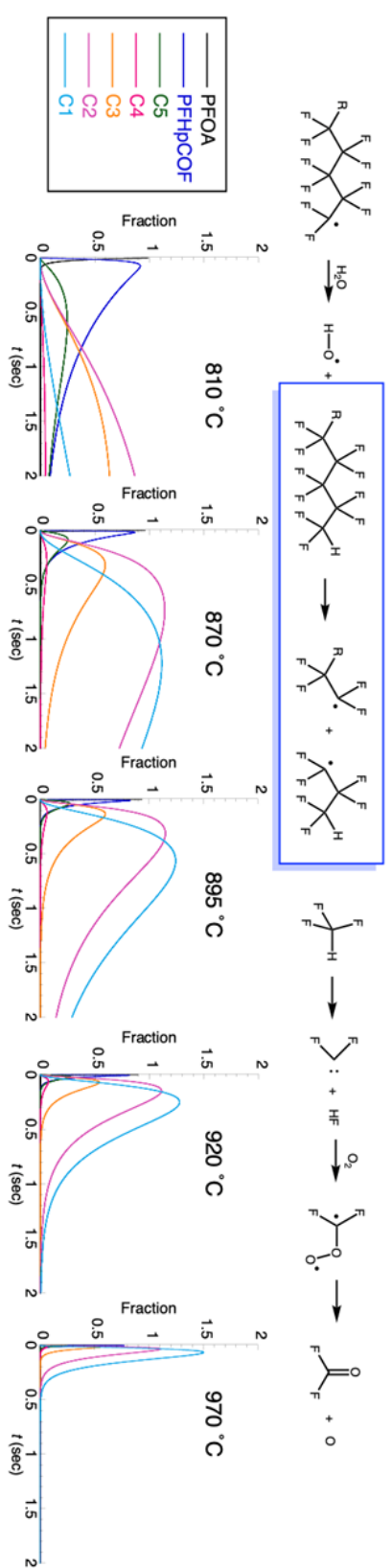
304 Given these high T_{99} temperatures, the cleavage of 1*H*-perfluoroalkanes and, if present,
305 perfluoroalkanes can be identified as the kinetic bottlenecks in the thermal gas-phase
306 decomposition of PFAS. Indeed, 1*H*-perfluoroalkanes were observed to be the dominant products
307 of incomplete thermal PFAS destruction in a recent pilot-scale AFFF decomposition study.¹⁰ Fully
308 fluorinated perfluoroalkanes were detected as minor products in the same pilot-scale study¹⁰ as
309 well as in a small-scale AFFF pyrolysis study.⁵³ The radical products of fluoroalkane C-C cleavage
310 then undergo the reactions discussed above (Fig. 3a).

311 **Kinetic Modeling.** As multiple potential parallel pathways exist, product distributions based on
312 predicted thermochemical parameters can be estimated using kinetic modeling.^{18,54} The important
313 question is at what temperature does complete mineralization occur and by which pathway. In Fig.
314 5 we compare two pathways for PFOA decomposition, a sequential carboxylic acid pathway and
315 a C-C bond cleavage pathway. PFOA was chosen as model species because among all PFAS
316 investigated in this study, PFCAs require the highest gas-phase decomposition temperatures and
317 can thus be seen as a worst-case scenario.

a)



b)



319 **Figure 5. Comparison of (a) a sequential carboxylic acid pathway with (b) a C-C bond**
320 **cleavage pathway for gas-phase PFOA decomposition as a function of temperature. The**
321 **kinetically limiting steps for the carboxylic acid path are α -HF elimination (blue box) and**
322 **\bullet OH addition to the acyl fluoride intermediates (green box). For the bond cleavage path, the**
323 **kinetically limiting steps are homolytic cleavage of various bonds in the carbon chain of the**
324 **initially formed perfluoroheptanoyl fluoride (PFHpCOF, green box) and cleavage of the 1H-**
325 **perfluoroalkane intermediates (blue box).**

326 As discussed above, PFOA initially decomposes via α -elimination to form a lactone
327 intermediate (Fig. 1), which rapidly decarbonylates into perfluoroheptanoyl fluoride (PFHpCOF,
328 Fig. 5a). In the sequential carboxylic acid pathway, subsequent PFHpCOF decomposition proceeds
329 by way of \bullet OH addition forming perfluoroheptanoic acid (PFHpA). This pathway then repeats to
330 generate acyl fluoride intermediates (R-COF) and PFCAs of increasingly shorter chain length. The
331 kinetic bottleneck in this pathway is the decomposition of the acyl fluoride species (T_{99} of 830-
332 880 °C versus T_{99} of 700 °C for α -elimination) as can be seen by the dominance of acyl fluorides
333 in the product distribution (Fig. 5a). Within the simulated temperature range of 810-970 °C, chosen
334 based on the pilot-scale study by Shields and colleagues,¹⁰ and at a hydroxyl radical concentration
335 representative of incineration conditions (3×10^{-6} atm), a significant fraction of PFAS remains up
336 to 920 °C, and only at 970 °C 97% of PFOA are completely destroyed via this pathway considering
337 a 2-second residence time.

338 In the C-C bond cleavage pathway (Fig. 5b), which is a unimolecular pathway independent
339 of any secondary species' concentration, the initially formed PFHpCOF undergoes chain rupture
340 in various places. This process generates C₁-C₅ perfluoroalkyl radicals, which then abstract
341 hydrogen to generate 1H-perfluororadicals in a repeating cycle that does not produce sequentially

342 shorter PFCAs. This pathway is kinetically preferred over the sequential carboxylic acid pathway:
343 at 920 °C only 0.3% of PFAS remains, and at 970 °C only 10⁻¹¹% of PFAS remains after 2 seconds.
344 We note that both pathways ultimately lead to the generation of carbonyl fluoride COF₂ (Fig. 5),
345 which rapidly decomposes in aqueous media (*T*₉₉ of 20 °C).

346 **Implications.** Our highly accurate coupled cluster calculations reveal that in the gas phase, i.e., in
347 the absence of heterogeneous catalysis on reactor, waste, ash or other surfaces, six out of eleven
348 PFAS classes investigated in this study undergo initial unimolecular head group loss, which
349 includes all perfluoroalkyl acids such as PFCAs and PFSAs. For all five fluorotelomers, however,
350 initial H abstraction from the telomeric functional group by hydroxyl radicals is more favorable
351 under incineration (combustion) conditions, which is then followed by rapid radical
352 decomposition. However, it is important to reiterate that changes in concentrations of radicals and
353 other reactive species in the gas phase may lead to changes in primary reaction mechanisms,
354 pathways, and kinetics. Therefore, even in the gas phase in the absence of catalytic processes, the
355 outcomes of thermal PFAS destruction can be expected to be specific to process conditions.

356 The major intermediates from thermal PFAS destruction are 1*H*-perfluoroalkanes,¹⁰ which
357 are formed when perfluoroalkyl radicals abstract hydrogen from hydrocarbon fuel and to a lesser
358 extent from water. Two implications of these findings are (1) that DREs calculated based on parent
359 PFAS removal are of little value and (2) that especially short-chain 1*H*-perfluoroalkanes are
360 suitable benchmark chemicals to assess whether a particular thermal process, reactor or facility is
361 capable of complete PFAS destruction.

362 Several previous bench-scale studies have reported thermal decomposition of parent PFAS
363 at temperatures hundreds of °C below the ones reported in this study.^{9,38,40,54} Such observations
364 are possible due to surface catalysis and other effects, but often do not capture the fate of volatile

365 PIDs generated. Fluorine mass balance closure is therefore not achieved, which is critical for the
366 assessment of destructive PFAS technologies⁵⁵ and should be the aim of future studies. It seems
367 prudent to ensure that a particular thermal process can sufficiently destroy 1*H*-perfluoroalkanes
368 within 2 seconds of gas residence time. Our kinetic calculations reveal that $\geq 99.99\%$ destruction
369 and removal of C₈ and shorter PFAS at the full scale are possible at temperatures around 950 °C.
370 In fact, hazardous waste incinerators typically operate at much higher temperatures around 1100
371 °C and commonly treat organic chemicals that require much higher temperatures than PFAS, such
372 as chlorobenzene ($T_{99} = 990$ °C), acetonitrile ($T_{99} = 1000$ °C), and naphthalene ($T_{99} = 1070$ °C).²⁰

373 It remains to be noted that safe and complete thermal PFAS destruction is a more complex
374 engineering problem than dialing in a temperature of ~ 950 °C at ≥ 2 seconds gas residence time.
375 One important factor is to optimize mixing in the reactor to ensure sufficient exposure to high
376 temperatures and to minimize pockets of depleted oxygen and other relevant reactants. Other
377 critical variables are waste stream composition, fuel:oxygen:PFAS ratio, and the presence of
378 fluorine scavenger(s), which are all related to the fact that many relevant reactions are bimolecular
379 with second-order kinetics, and therefore concentration-dependent. For instance, a very limited
380 number of experimental studies^{38,56} have reported the generation of tetrafluoromethane, a potent
381 greenhouse gas, through recombination of CF₃ with fluorine. As discussed above, CF₄ destruction
382 requires extremely high temperatures > 1400 °C because high-barrier C-F bond dissociation is the
383 only decomposition mechanism. Preventing tetrafluoromethane formation should thus be a main
384 priority during process development and optimization, and can be achieved by (1) providing
385 sufficient hydrogen donors such as hydrocarbons and water, (2) lowering PFAS and thus F
386 concentrations in the feed, and/or (3) adding fluorine scavengers such as lime to the feed. These
387 best practices are imperative for safe thermal destruction of PFAS.

388

389

390 **AUTHOR INFORMATION**

391 **Corresponding Author**

392 *(A.K.R.) E-mail: anthony.rappe@colostate.edu. Phone: +1-970-491-6292.

393 **Notes**

394 The authors declare no competing financial interest.

395

396 **ASSOCIATED CONTENT**

397 **Supporting Information.** The Supporting Information is available free of charge at...

398 Computational details; free energy corrections for incineration, thermal oxidation, and oxygen-

399 depleted conditions; tabulated T_{99} values; temperature plots for individual PFAS and thermal

400 decomposition intermediates.

401

402 **ACKNOWLEDGMENTS**

403 Financial support for this research was provided by the U.S. Department of Defense's Strategic

404 Environmental Research and Development Program (SERDP) under Project ER21-1019.

405

406 **REFERENCES**

407 (1) Tokranov, A. K.; Nishizawa, N.; Amadei, C. A.; Zenobio, J. E.; Pickard, H. M.; Allen, J. G.;

408 Vecitis, C. D.; Sunderland, E. M. How Do We Measure Poly- and Perfluoroalkyl Substances

409 (PFASs) at the Surface of Consumer Products? *Environ. Sci. Technol. Lett.* **2019**, *6*, 38-43.

- 410 (2) Wang, Z.; DeWitt, J. C.; Higgins, C. P.; Cousins, I. T. A Never Ending Story of Per- and
411 Polyfluoroalkyl Substances (PFASs)? *Environ. Sci. Technol.* **2017**, *51*, 2508-2518.
- 412 (3) Buck, R.C.; Franklin, J.; Berger, U.; Conder, J.M.; Cousins, I.T.; de Voogt, P.; Jensen, A.A.;
413 Kannan, K.; Mabury, S.A.; van Leeuwen, S.P.J. Perfluoroalkyl and polyfluoroalkyl
414 substances in the environment: terminology, classification, and origins. *Integr. Environ.*
415 *Assess. Manage.* **2011**, *7*, 513-541.
- 416 (4) Cousins, I.T.; DeWitt, J.C.; Glüge, J.; Goldenman, G.; Herzke, D.; Lohmann, R.; Ng, C.A.;
417 Scheringer, M.; Wang, Z. The high persistence of PFAS is sufficient for their management
418 as a chemical class. *Environ. Sci. Process Impacts* **2020**, *22*, 2307-2312.
- 419 (5) Tsang, W.; Burgess Jr., D.R.; Babushok, V. On the Incinerability of Highly Fluorinated
420 Organic Compounds. *Combust. Sci. and Tech.* **1998**, *139*, 385-402.
- 421 (6) Wang, J.; Lin, Z.; He, X.; Song, M.; Westerhoff, P.; Doudrick, K.; Hanigan, D. Critical
422 Review of Thermal Decomposition of Per- and Polyfluoroalkyl Substances: Mechanisms
423 and Implications for Thermal Treatment Processes. *Environ. Sci. Technol.* **2022**, *56*, 5355-
424 5370.
- 425 (7) Hall, H.; Moodie, D.; Vero, C. PFAS in Biosolids: A Review of International Regulations.
426 *Water e-Journal* **2020**, *5*, 4. <https://doi.org/10.21139/wej.2020.026>.
- 427 (8) United States Department of Defense, Office of the Assistant Secretary of Defense for
428 Energy, Installations, and Environment. Incineration Moratorium. Report to Congress. 03
429 February 2023, Washington, DC, USA.
- 430 (9) Xiao, F.; Challa Sasi, P.; Yao, B.; Kubatova, A.; Golovko, S.A.; Golovko, M.Y.; Soli, D.
431 Thermal Stability and Decomposition of Perfluoroalkyl Substances on Spent Granular
432 Activated Carbon. *Environ. Sci. Technol. Lett.* **2020**, *7*, 343-350.

- 433 (10) Shields, E.P.; Krug, J.D.; Roberson, W.R.; Jackson, S.R.; Smeltz, M.G.; Allen, M.R.;
434 Burnette, R.P.; Nash, J.T.; Virtaranta, L.; Preston, W. et al. Pilot-Scale Thermal Destruction
435 of Per-and Polyfluoroalkyl Substances in a Legacy Aqueous Film Forming Foam. *ACS EST*
436 *Engg.* **2023**, 3 (9), 1308-1317.
- 437 (11) Mattila, J.M.; Krug, J.D.; Roberson, W.R.; Burnette, R.P.; S. McDonald; Virtaranta, L.;
438 Offenberg, J.H.; Linak, W.P. Characterizing Volatile Emissions and Combustion
439 Byproducts from Aqueous Film-Forming Foams Using Online Chemical Ionization Mass
440 Spectrometry. *Environ. Sci. Technol.* **2024**, 58 (8), 3942-3952.
- 441 (12) Blotevogel, J.; Giraud, R.J.; Rappé, A.K. Incinerability of PFOA and HFPO-DA:
442 Mechanisms, Kinetics, and Thermal Stability Ranking. *Chemical Engineering Journal* **2023**,
443 457, 141235.
- 444 (13) Watanabe, N.; Takata, M.; Takemine, S.; Yamamoto, K. Thermal mineralization behavior
445 of PFOA, PFHxA, and PFOS during reactivation of granular activated carbon (GAC) in
446 nitrogen atmosphere. *Environ. Sci. Pollut. Res.* **2018**, 25, 7200-7205.
- 447 (14) Kundu, S.; Patel, S.; Halder, P.; Patel, T.; Hedayati Marzbali, M.; Pramanik, B. K.; Paz-
448 Ferreira, J.; de Figueiredo, C. C.; Bergmann, D.; Surapaneni, A.; Megharaj, M.; Shah,
449 K. Removal of PFASs from biosolids using a semi-pilot scale pyrolysis reactor and the
450 application of biosolids derived biochar for the removal of PFASs from contaminated
451 water. *Environmental Science: Water Research & Technology* **2021**, 7 (3), 638-649.
- 452 (15) Feng, Y.; Liu, L.; Wang, J.T.; Huang, H.; Guo, Q.X. Assessment of experimental bond
453 dissociation energies using composite ab initio methods and evaluation of the performances
454 of density functional methods in the calculation of bond dissociation energies. *J. Chem. Inf.*
455 *Comput. Sci.* **2003**, 43, 2005-2013.

- 456 (16) Truhlar, D.; Garrett, B. Variational Transition State Theory. *Annu. Rev. Phys.*
457 *Chem.* **1984**, *35*, 159-189.
- 458 (17) Bao, J.L.; Zhang, X.; Truhlar, D.G. Barrierless association of CF₂ and dissociation of C₂F₄
459 by variational transition-state theory and system-specific quantum Rice–Ramsperger–Kassel
460 theory. *Proc. Natl. Acad. Sci. U.S.A.* **2016**, *113*, 13606-13611.
- 461 (18) Altarawneh, M., Almatarneh, M.H., Dlugogorski, B.Z. Thermal decomposition of
462 perfluorinated carboxylic acids: kinetic model and theoretical requirements for PFAS
463 incineration. *Chemosphere* **2022**, *286*, 131685.
- 464 (19) Dellinger, B.; Taylor, P.H.; Lee, C.C. Full-scale evaluation of the thermal stability-based
465 hazardous organic waste incinerability ranking. *Air & Waste* **1993**, *43*, 203-207.
- 466 (20) Taylor, P.H.; Dellinger, B.; Lee, C.C. Development of a Thermal Stability Based Ranking
467 of Hazardous Organic Compound Incinerability. *Environ. Sci. Technol.* **1990**, *24*, 316-328.
- 468 (21) Adi, M. A.; Altarawneh, M. Thermal decomposition of heptafluoropropylene-oxide-dimer
469 acid (GenX). *Chemosphere* **2022**, *289*, 133118.
- 470 (22) Khan, M.Y.; So, S.; da Silva, G. Decomposition kinetics of perfluorinated sulfonic acids.
471 *Chemosphere* **2020**, *238*, 124616.
- 472 (23) Altarawneh, M.A. Chemical Kinetic Model for the Decomposition of Perfluorinated
473 Sulfonic Acids. *Chemosphere* **2021**, *263*, 128256.
- 474 (24) Krishnan, R.; Binkley, J. S.; Seeger, R.; Pople, J. A. Self-consistent molecular orbital
475 methods. XX. A basis set for correlated wave functions. *J. Chem. Phys.* **1980**, *72*, 650-654.
- 476 (25) Chai, J.-D; Head-Gordon, M. Systematic optimization of long-range corrected hybrid
477 density functionals. *J. Chem. Phys.* **2008**, *128*, 084106.

- 478 (26) Frisch, M. J.; Trucks, G. W.; Schlegel, H. B.; Scuseria, G. E.; Robb, M. A.; Cheeseman, J.
479 R.; Scalmani, G.; Barone, V.; Petersson, G. A.; Nakatsuji, H.; Li, X.; Caricato, M.; Marenich,
480 A. V.; Bloino, J.; Janesko, B. G.; Gomperts, R.; Mennucci, B.; Hratchian, H. P.; Ortiz, J. V.;
481 Izmaylov, A. F.; Sonnenberg, J. L.; Williams-Young, D.; Ding, F.; Lipparini, F.; Egidi, F.;
482 Goings, J.; Peng, B.; Petrone, A.; Henderson, T.; Ranasinghe, D.; Zakrzewski, V. G.; Gao,
483 J.; Rega, N.; Zheng, G.; Liang, W.; Hada, M.; Ehara, M.; Toyota, K.; Fukuda, R.; Hasegawa,
484 J.; Ishida, M.; Nakajima, T.; Honda, Y.; Kitao, O.; Nakai, H.; Vreven, T.; Throssell, K.;
485 Montgomery, J. A., Jr.; Peralta, J. E.; Ogliaro, F.; Bearpark, M. J.; Heyd, J. J.; Brothers, E.
486 N.; Kudin, K. N.; Staroverov, V. N.; Keith, T. A.; Kobayashi, R.; Normand, J.;
487 Raghavachari, K.; Rendell, A. P.; Burant, J. C.; Iyengar, S. S.; Tomasi, J.; Cossi, M.; Millam,
488 J. M.; Klene, M.; Adamo, C.; Cammi, R.; Ochterski, J. W.; Martin, R. L.; Morokuma, K.;
489 Farkas, O.; Foresman, J. B.; Fox, D. J. Gaussian 16. 2016. Gaussian, Inc., Wallingford CT.
- 490 (27) Eichkorn, K.; Treutler, O.; Öhm, H.; Häser, M.; Ahlrichs, R. Auxiliary basis sets to
491 approximate Coulomb potentials. *Chem. Phys. Lett.* **1995**, *240*, 283-290.
- 492 (28) Weigend, F.; Häser, M.; Patzelt, H.; Ahlrichs, R. RI-MP2: optimized auxiliary basis sets and
493 demonstration of efficiency. *Chem. Phys. Lett.* **1998**, *294*, 143-152.
- 494 (29) Riplinger, C.; Neese, F. An efficient and near linear scaling pair natural orbital based local
495 coupled cluster method. *J. Chem. Phys.* **2013**, *138*, 034106.
- 496 (30) Saitow, M.; Becker, U.; Riplinger, C.; Valeev, E.F.; Neese, F. A new near-linear scaling,
497 efficient and accurate, open-shell domain-based local pair natural orbital coupled cluster
498 singles and doubles theory. *J. Chem. Phys.* **2017**, *146*, 164105.
- 499 (31) Neese, F. The ORCA program system. *WIREs Comput. Mol. Sci.* **2012**, *2*, 73-78.

- 500 (32) Martin, J. M. L. Basis set convergence study of the atomization energy, geometry, and
501 anharmonic force field of SO₂: The importance of inner polarization functions. *J. Chem.*
502 *Phys.* **1998**, *108*, 2791-2800.
- 503 (33) Goodwin, D.G; Moffat, H.K.; Schoegl, I.; Speth, R.; Weber, B.W. Cantera: An object-
504 oriented software toolkit for chemical kinetics, thermodynamics, and transport processes.
505 <https://www.cantera.org>, 2023. Version 3.0.0. doi:10.5281/zenodo.8137090.
- 506 (34) Krusic, P.J.; Marchione, A.A.; Roe, D.C. Gas-phase NMR studies of the thermolysis of
507 perfluorooctanoic acid. *Journal of Fluorine Chemistry* **2005**, *126*, 1510-1516.
- 508 (35) Alinezhad, A.; Shao, H.; Litvanova, K.; Sun, R.; Kubatova, A.; Zhang, W.; Li, Y.; Xiao, F.
509 Mechanistic investigations of thermal decomposition of perfluoroalkyl ether carboxylic
510 acids and short-chain perfluoroalkyl carboxylic acids. *Environmental Science & Technology*
511 **2023**, *57*, 8796-8807.
- 512 (36) Weber, N.H.; Dixon, L.J.; Stockenhuber, S.P.; Grimison, C.C.; Lucas, J.A.; Mackie, J.C.;
513 Stockenhuber, M.; Kennedy, E.M. Thermal decomposition of PFOA: Influence of reactor
514 and reaction conditions on product formation. *Chem. Eng. Sci.* **2023**, *278*, 118924.
- 515 (37) Ge, Y.; Liu, Z.-Z.; Liu, H.-X.; Feng, J.-K.; Liu, D.-S.; Ge, X.-W. Theoretical Study on the
516 Degradation Reaction Mechanism of Elimination Hydrogen Fluoride from
517 Perfluoropropionic Acid. *Computational and Theoretical Chemistry* **2014**, *1029*, 33-40.
- 518 (38) Wang, J.; Song, M.; Abusallout, I.; Hanigan, D. Thermal Decomposition of Two Gaseous
519 Perfluorocarboxylic Acids: Products and Mechanisms. *Environ. Sci. Technol.* **2023**, *57*,
520 6179-6187.

- 521 (39) Weber, N.H.; Delva, C.S.; Stockenhuber, S.P.; Grimison, C.C.; Lucas, J.A.; Mackie, J.C.;
522 Stockenhuber, M.; and Kennedy, E.M. Thermal Mineralization of Perfluorooctanesulfonic
523 Acid (PFOS) to HF, CO₂, and SO₂. *Ind. Eng. Chem. Res.* **2023**, *62*, 881-892.
- 524 (40) Xiao, F.; Sasi, P. C.; Yao, B.; Kubátová, A.; Golovko, S. A.; Golovko, M. Y.; Soli, D.
525 Thermal Decomposition of PFAS: Response to Comment on “Thermal Stability and
526 Decomposition of Perfluoroalkyl Substances on Spent Granular Activated Carbon.
527 *Environmental Science & Technology Letters* **2021**, *8*, 364-365.
- 528 (41) Doolan, K.R.; Mackie, J.C.; Reid C.R. High Temperature Kinetics of the Thermal
529 Decomposition of the Lower Alkanoic Acids. *Int. J. Chem. Kin.* **1986**, *18*, 575-596.
- 530 (42) Namysl, S.; Pelucchi, M.; Herbinet, O.; Frassoldati, A.; Faravelli, T.; Battin-Leclerc, F.A.
531 First evaluation of butanoic and pentanoic acid oxidation kinetics. *Chemical Engineering*
532 *Journal* **2019**, *373*, 973-984.
- 533 (43) Clark, J. M.; Nimlos, M. R.; Robichaud, D. J. Comparison of Unimolecular Decomposition
534 Pathways for Carboxylic Acids of Relevance to Biofuels. *J. Phys. Chem. A.* **2014**, *118*, 260-
535 274.
- 536 (44) Tseng, N.; Wang, N.; Szostek, B.; Mahendra, S. Biotransformation of 6:2 fluorotelomer
537 alcohol (6:2 FTOH) by a wood-rotting fungus. *Environ. Sci. Technol.* **2014**, *48*, 4012-4020.
- 538 (45) Heufer, K. A.; Sarathy, S. M.; Curran, H. J.; Davis, A. C.; Westbrook, C. K.; Pitz, W. J.
539 Detailed Kinetic Modeling Study of *n*-Pentanol Oxidation. *Energy Fuels* **2012**, *26*, 6678-
540 6685.
- 541 (46) Ainagos, A.F. Mechanism and Kinetics of Pyrolysis of Perfluorohexane. *Kinet. Catal.* **1991**,
542 *32*, 720-725.

- 543 (47) Hansen, A. S.; Bhagde, T.; Moore III, K. B.; Moberg, D. R.; Jasper, A. W.; Georgievskii,
544 Y.; Vansco, M. F.; Klippenstein, S. J.; Lester, M. K. Watching a hydroperoxyalkyl radical
545 (\bullet QOOH) dissociate. *Science* **2021**, *373*, 679-682.
- 546 (48) Yu, H.; Kennedy, E. M.; Ong, W.-H.; Mackie, J. C.; Han, W.; Dlugogorski, B. Z.
547 Experimental and Kinetic Studies of Gas-phase Pyrolysis of *n*-C₄F₁₀. *Ind. Eng. Chem. Res.*
548 **2008**, *47*, 2579-2584.
- 549 (49) Bezuidenhoudt, A.; Sonnendecker, P. W.; Crouse, P. L. Temperature and pressure effects on
550 the product distribution of PTFE pyrolysis by means of qualitative, in-line FTIR analysis.
551 *Polymer Degradation and Stability* **2017**, *142*, 79-88.
- 552 (50) Conesa, J. A.; Font R. Polytetrafluoroethylene Decomposition in Air and Nitrogen. *Poly.*
553 *Eng. Sci.* **2001**, *41*, 2137-2147.
- 554 (51) Tschuikow-Roux, E. Kinetics of the Thermal Decomposition of C₂F₆ in the Presence of H₂
555 at 1300°-1600°K. *J. Chem. Phys.* **1965**, *43*, 2251-2256.
- 556 (52) Cobos, C.J.; Croce, A.E.; Luther, K.; Troe, J. Temperature and Pressure Dependence of the
557 Reaction 2CF₃ (+ M) ↔ C₂F₆ (+ M). *J. Phys. Chem. A* **2010**, *114*, 4748-4754.
- 558 (53) Yao, B.; Sun, R.; Alinezhad, A.; Kubatova, A.; Simcik, M. F.; Guan, X.; Xiao, F. The first
559 quantitative investigation of compounds generated from PFAS, PFAS-containing aqueous
560 film-forming foams and commercial fluorosurfactants in pyrolytic processes. *J. Hazard.*
561 *Mater.* **2022**, *436*, 129313.
- 562 (54) Weber, N. H.; Stockenhuber, S. P.; Delva, C. S.; Abu Fara, A.; Grimison, C. C.; Lucas, J.
563 A.; Mackie, J. C.; Stockenhuber, M.; Kennedy, E. M. Kinetics of Decomposition of PFOS
564 Relevant to Thermal Desorption Remediation of Soils. *Ind. Eng. Chem. Res.* **2021**, *60*, 9080-
565 9087.

- 566 (55) Smith, S.J.; Lauria, M.; Higgins, C.P.; Pennell, K.D.; Blotevogel, J.; Arp, H.P.H. The Need
567 to Include a Fluorine Mass Balance in the Development of Effective Technologies for PFAS
568 Destruction. *Environ. Sci. Technol.* **2024**, *58*, 2587-2590.
- 569 (56) Krug, J. D.; Lemieux, P. M.; Lee, C. W.; Ryan, J. V.; Kariher, P. H.; Shields, E. P.;
570 Wickersham, L. C.; Denison, M. K.; Davis, K. A.; Swensen, D. A.; Burnette, R. P.; Wendt,
571 J. O. L.; Linak, W. P. Combustion of C₁ and C₂ PFAS: Kinetic modeling and experiments.
572 *J. Air Waste Manag. Assoc.* **2022**, *72* (3), 256–270.